

Electric flight scheduling with battery-charging and battery-swapping opportunities

Mitici, M.A.; Ramos Pereira, M.; Oliviero, F.

DOI

[10.1016/j.ejtl.2022.100074](https://doi.org/10.1016/j.ejtl.2022.100074)

Publication date

2022

Document Version

Final published version

Published in

EURO Journal on Transportation and Logistics

Citation (APA)

Mitici, M. A., Ramos Pereira, M., & Oliviero, F. (2022). Electric flight scheduling with battery-charging and battery-swapping opportunities. *EURO Journal on Transportation and Logistics*, 11, Article 100074. <https://doi.org/10.1016/j.ejtl.2022.100074>

Important note

To cite this publication, please use the final published version (if applicable).
Please check the document version above.

Copyright

Other than for strictly personal use, it is not permitted to download, forward or distribute the text or part of it, without the consent of the author(s) and/or copyright holder(s), unless the work is under an open content license such as Creative Commons.

Takedown policy

Please contact us and provide details if you believe this document breaches copyrights.
We will remove access to the work immediately and investigate your claim.



Electric flight scheduling with battery-charging and battery-swapping opportunities

Mihaela Mitici^{*}, Madalena Pereira, Fabrizio Oliviero

Faculty of Aerospace Engineering, Delft University of Technology, HS 2926 Delft, the Netherlands

ARTICLE INFO

Keywords:

Scheduling
Electric aircraft
Linear optimization
Battery charge and swap

ABSTRACT

With the current advances in aircraft design and Lithium-Ion batteries, electric aircraft are expected to serve as a replacement for conventional, short-range aircraft. This paper addresses the main operational challenges for short-range flights operated with electric aircraft: determining the investment needs for a fleet of electric aircraft, and the logistics of charging stations and swap batteries required to support these flights. A mixed-integer linear program with two phases is proposed. In the first phase, a schedule for flight and battery recharge is developed for a fleet of electric aircraft. In the second phase, optimal times for battery charging are determined, together with an optimal sizing of the number of charging stations and swap batteries. We illustrate our model for short-range flights to and from an European airport and for an electric aircraft designed based on the operational characteristics of a conventional, narrow-body aircraft.

1. Introduction

It is estimated that the CO₂ emissions generated by aviation are 2.5–3% of the anthropogenic CO₂, causing 5–9% of the anthropogenic radiative forcing (Lee et al., 2009). To address this, the EU has signed in 2020 The European Green Deal Investment Plan (Tamma et al., 2020), which aims to achieve a climate neutral EU by 2050 by *investing in environmentally-friendly technologies, and rolling out cleaner, cheaper and healthier forms of private and public transport*. A promising cleaner means of transport are the electric or hybrid-electric aircraft (e-AC), which are expected to serve as a replacement for conventional aircraft. One such example is E-Fan X aircraft, introduced in 2017 by Airbus. However, due to the intrinsic design challenges related to electric powered-aircraft, it is expected that electric aircraft will first be used for short-range only.

From an operational point of view, however, replacing conventional aircraft with e-AC for short-range flights poses several challenges. First, how many electric aircraft should an airline acquire to satisfy a given flight demand? Second, the aircraft are expected to be charged at the airport, using charging stations and/or use fully-charged, spare batteries. Also here, it is of interest to understand how many charging stations would an airport need to sustain electric flights, as well as how many spare batteries are needed. Third, it is of interest to understand how should the e-AC be scheduled for flight and battery recharging.

We address these operational challenges by proposing a novel, two-

phase mixed-integer linear programming (MILP) model to schedule electric aircraft for short-range round-trip flights (missions) to and from a reference airport. Since it is expected that initially only large airports will have the necessary infrastructure to support electric flights, we assume that the battery management (battery charging, swapping) takes place at a hub-reference airport where round-trip flight originate from. The first phase of the optimization determines an optimal investment for a fleet of electric aircraft, given a flight demand, as well as an optimal sequence of missions and aircraft battery recharging events. In the second phase, we apply time discretization and determine i) optimal times to start battery charging, ii) at which charging station to perform the charging, and iii) what is a minimum number of spare batteries needed to conduct the considered missions. By applying time discretization only in the second phase, the problem becomes computationally tractable. We illustrate our model for short-range flights to and from a hub airport. Since charging specifications are not yet available for electric aircraft, in this paper we consider charging specifications of an e-AC designed based on the operational characteristics of a regional carrier Embraer E175.

Regarding contributions from a practical point of view, by determining an optimal number of charging stations and spare batteries for a given flight demand, our model provides airports with insights into infrastructure and logistics requirements for electric flights. Also, our model provides airlines with support in the acquisition of a fleet of electric aircraft to satisfy a specific flight demand. Nevertheless, our

^{*} Corresponding author.

E-mail address: m.a.mitici@tudelft.nl (M. Mitici).

<https://doi.org/10.1016/j.ejtl.2022.100074>

Received 24 December 2020; Received in revised form 23 December 2021; Accepted 9 February 2022

Available online 16 February 2022

2192-4376/© 2022 The Author(s). Published by Elsevier B.V. on behalf of Association of European Operational Research Societies (EURO). This is an open access

article under the CC BY-NC-ND license (<http://creativecommons.org/licenses/by-nc-nd/4.0/>).

approach can be considered for other electric means of transport, where the logistics of recharging options are of interest.

The remainder of the paper is structured as follows. In Section 2 we discuss prior work on scheduling of electric vehicles. In Section 3 we describe the problem of scheduling electrical aircraft for missions, with the possibility to charge batteries at a charging station or to swap batteries. In Section 4 we specify a two-phase optimisation model for our electric aircraft scheduling problem. In Section 5 we introduce a battery charging and discharging model for the e-AC considered, based on a conventional, narrow-body aircraft. In Section 6 we illustrate our model for short-range flights arriving to and departing from a large European airport.

2. Prior work and contributions

In the past years, several studies have addressed the Electric Vehicle Scheduling Problem (e-VSP) (Adler and Mirchandani, 2016; Wen et al., 2016; Emde et al., 2018; Rinaldi et al., 2018; Chao and Xiaohong, 2013; Li, 2013). In these studies, assumptions are made regarding the charging location and the duration of the charging. In (Adler and Mirchandani, 2016; Justin et al., 2020), the authors assume that the batteries of the electric vehicles can be charged at several locations. In comparison, we consider electric aircraft that can charge their batteries at an origin airport, where round-trip flights originate from. This is relevant for current aircraft operations, where only a few airports are envisioned to be able to support electric flights. Regarding the battery charging duration, instant charging is considered in (Adler and Mirchandani, 2016; Rinaldi et al., 2018), whereas (Li, 2013) assumes a fixed charging duration, regardless of the residual battery energy. In (Wen et al., 2016; Emde et al., 2018) the charging duration is assumed to increase linearly with the required charge amount. In comparison, we consider that the charging duration follows a bi-linear charging profile, where for a charge of more than 90% of the battery capacity, the slope of the charging profile decreases, i.e., slow charging. Also, we take into account the residual battery charge before re-charge. In fact, a re-charge/swap can be postponed if the residual battery charge is sufficient to perform a new mission.

In general, electric vehicles scheduling considers only single trips (Adler and Mirchandani, 2016; Wen et al., 2016; Rinaldi et al., 2018; Chao and Xiaohong, 2013; Li, 2013; Kleinbekman et al., 2019; Justin et al., 2020), except for (Emde et al., 2018) which considers round trips, as in the case of our paper. In (Emde et al., 2018) the authors schedule a fleet of electric vehicles to timetabled milk-run trips. The proposed model is solved using two heuristics. In contrast, in this paper we obtain an optimal solution in a short computational time by modeling the problem in 2 optimization phases, which makes the problem computationally tractable. In (Justin et al., 2020) a network of airports is assumed. After every flight the battery of the aircraft can be recharged at its destination airport.

e-VSP with battery swapping, instead of battery charging, is considered in (Chao and Xiaohong, 2013; Sun et al., 2019). The swapped batteries need to be recharged so that they can be reused and a minimal number of required spare batteries is determined. In (Justin et al., 2020) a pool of spare batteries is considered, which can be either swapped or recharged in order to minimize the peak-power draw from the grid and capital expenditures. In (Verma, 2018) an heuristic is proposed for the electric vehicle routing problem with both battery charging and battery swapping opportunities. Similarly, we consider a mix of both battery swapping and charging at a charging station.

In (Wen et al., 2016; Emde et al., 2018; Kleinbekman et al., 2019) the time required to charge a battery evolves linearly with the remaining State-of-Charge (SOC) of the battery. In contrast, in this paper, we assume a bi-linear charging function such that the charging duration increases significantly when charging above 90% of the battery capacity, which reflects the charging behaviour of Li-Ion battery technologies that are nowadays used for automotive applications.

3. Problem description

We consider a given set M of short-range missions, $|M| = m$, that are scheduled during one day of operations (see Fig. 1). A mission is defined to be a round trip from a reference-origin airport to a destination airport and back to the origin airport. Each mission has a departure time, t^d , an arrival time, t^a , $t^a > t^d$, and a range, i.e. flown distance (km) between takeoff and landing. We consider a homogeneous fleet of e-AC that fly the set of missions M . Each aircraft is assumed to be equipped with one battery of capacity Q kWh. At the origin airport, there is a set of charging stations and a set of identical, fully-charged, spare batteries which the e-AC can use. We consider a stock of identical batteries to be the total number of batteries i) inside the aircraft plus ii) spare batteries, available at the airport. If a charging station is used, then only one aircraft at a time can recharge its battery at this station. The size of the e-AC fleet, the number of charging stations and the number of spare batteries are to be determined by our proposed model.

To fulfill a mission with an e-AC, the battery inside this e-AC uses an amount of electrical energy. Thus, after a mission is completed, this battery's *State of Charge*, SOC, decreases. We assume that the amount of energy decreases according to a linear function of the range of the completed mission. We keep track of the SOC of the e-AC upon mission completion. When we begin a battery recharge at a charging station, we initiate this recharging taking into account the residual SOC. Also, the battery charges only the required energy to fulfill the newly assigned mission. For example, let us assume that, after an e-AC completes a mission, its remaining SOC is 35% of the battery capacity. A new mission is assigned to this aircraft, which requires 40% of the battery capacity. It is decided to charge the battery at a charging station. Assuming a safety margin $SF = 20\%$, the battery is then charged for the new mission an addition of $5\% + 20\%$ of the battery capacity to a final SOC of $35\% + 5\% + 20\%$ of its capacity.

After completing a mission, the e-AC can i) recharge its battery using a charging station located at the origin airport, ii) swap its battery with a fully-charged, spare battery if any is available, or iii) keep its current battery without recharging, provided there is enough SOC. Charging the aircraft's battery at a charging station is time-consuming and makes the e-AC unavailable during the charging period. Lastly, we ensure that at the end of a day of operations, all batteries (inside the aircraft and spares) are fully charged, so that at the beginning of a new day of operations, all batteries are fully charged.

We are interested in determining how many e-AC should the airline acquire, given aircraft acquisition costs and flight demand, as well as how to schedule e-AC for missions and battery recharging events (how many charging stations, how many spare batteries and when to charge/swap batteries).

As an example, Fig. 2 shows four missions, where mission $i \in \{1, 2, 3, 4\}$ has departure and arrival time at the origin airport t_i^d and t_i^a , respectively. We denote by a_{ij} the turnaround time between two missions i and j , $i, j \in \{1, \dots, 4\}$, $i \neq j$. Two missions i and j cannot be consecutively executed in the order i is immediately succeeded by j in the case: (a) the first mission i departs at a later time than the second mission j , (b) the aircraft is executing mission i at the time of the departure of the second mission j , i.e., $t_i^a > t_j^d$, (c) after the completion of the first mission i , the aircraft does not have sufficient time to carry out the necessary battery recharge/swap so that enough energy is available to execute the second mission j . In Fig. 2, missions 1 and 3 are an example of case (a). Missions 1 and 2 illustrate case (b) since they overlap. Lastly, missions 3 and 4 illustrate case (c). Even though $t_3^a < t_4^d$, the required turnaround time, a_{34} , between missions 3 and 4, prevents the aircraft from executing mission 4 at t_4^d , i.e., $t_3^a + a_{34} > t_4^d$.

We further discuss case (c) considering battery constraints. Let us assume that missions 3 and 4 in Fig. 2 require 70% and 80% of the e-AC battery capacity to be executed, respectively. Let us also assume that i) the e-AC is fully charged before performing mission 3, ii) between the

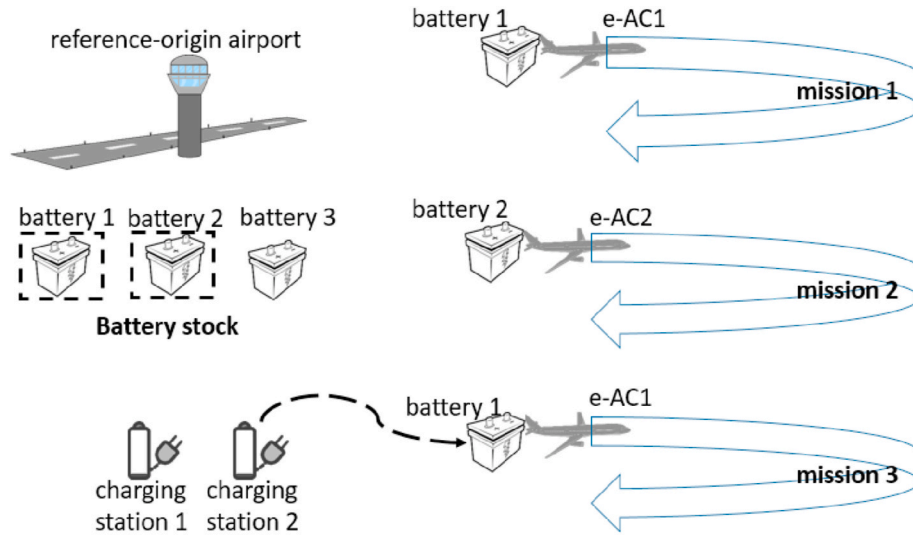


Fig. 1. Example of e-AC to missions assignment, where there are $m = 3$ missions. For the 3 missions, we have a fleet of 2 e-AC, a stock of 3 identical batteries (2 batteries inside the 2 aircraft and 1 spare battery) and 2 identical charging stations. The set of 3 missions is known, while the aircraft fleet size, the size of the battery stock and the number of charging stations are to be determined by our proposed model.

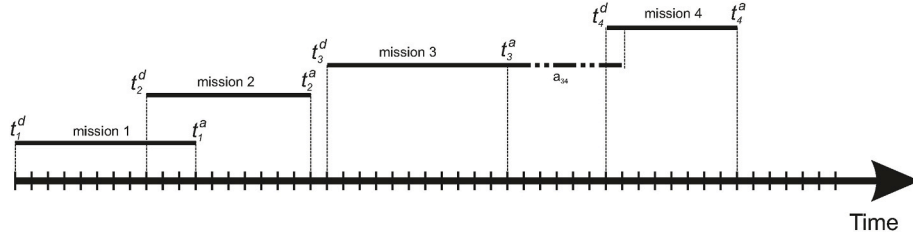


Fig. 2. Example of constraining factors for the assignment of e-AC to missions.

arrival of mission 3 and the departure of mission 4 there is a time period of only 30min and, iii) battery charging is performed at 1% per minute. Thus, if the e-AC that executed mission 3 would also be assigned to mission 4 (turnaround time of 30min), then it would have to charge $80 - (100 - 70) = 50\%$. Since the charging would take 50min to be completed, but only 30min turnaround time is available between missions 3 and 4, the e-AC cannot execute mission 4 immediately after mission 3.

4. e-AC scheduling problem with battery-charging and battery-swapping opportunities

We consider a two-phase approach for the e-AC scheduling problem with battery-charging and battery-swapping opportunities.

The first phase of the optimization problem consists in i) assigning e-AC to missions and ii) a decision is made whether to swap the battery of the e-AC or to charge this battery at a charging station (see Fig. 3). These

decisions are driven by the costs needed to acquire a fleet of electric aircraft to satisfy a given flight demand (missions).

In this phase we only decide whether a battery charge/swap occurs during turnaround times (i.e., time between missions), but we do not determine the exact time when the charging starts or when the swap occurs. The output of this phase is: the size of the fleet of e-AC, the assignment of e-AC to missions and, given this assignment, the decision to charge/swap the battery of an e-AC during its turnaround time.

In the second phase (see Fig. 4), we take the result of the first phase as an input and determine i) at which charging station to charge a battery and at what time to start this charge (the battery charging is either inside the aircraft or is available at the airport as a spare, depleted battery), ii) what is the minimum number of charging stations and spare batteries needed to satisfy all battery charges and swaps scheduled in the first phase.

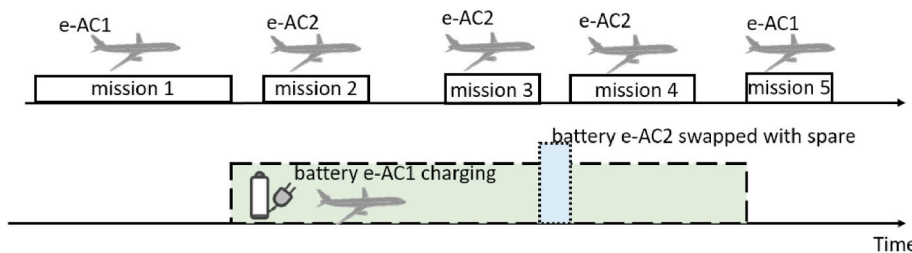


Fig. 3. Example of a first-phase solution, with five missions to be carried out: e-AC1 is assigned to missions 1 and 5, e-AC2 is assigned to missions 2, 3, 4. Following the e-AC-to-mission assignment, the turnaround time for e-AC1 is the time between t_1^a and t_5^d , i.e., $a_{15} = t_5^d - t_1^a$. For e-AC1, the battery is charging at a station during a_{15} . At this phase we do not know when the charging starts during the turnaround time a_{15} . However, by deciding to charge during a_{15} , we ensured that a_{15} is at least as large as the time needed to charge for mission 5. For e-AC2, the battery is swapped with a spare one during its turnaround time

a_{34} . We assume a fixed battery swap time. By deciding to swap the battery during a_{34} , we ensured that a_{34} is at least as large as the battery swapping time.

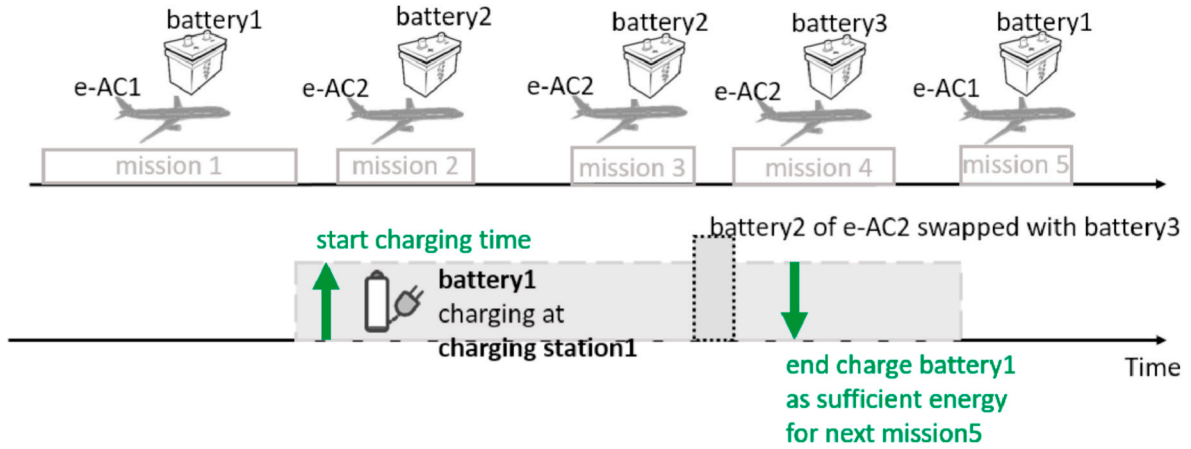


Fig. 4. Example of a second-phase solution. Following the first-phase solution (see Fig. 3), the charging start time for battery 1 inside e-AC1 is determined. This start time is within turnaround time a_{15} of e-AC1. To perform all 5 missions, a minimum of one spare battery (a battery stock of three batteries) and one charging station is required.

4.1. First phase: fleet sizing, e-AC-to-mission and battery-to-recharging assignment

We first introduce the following notation. Let V denote a set of e-AC, $|V| = v$. We will show below how to initialize the value v . Let mission $i \in M$ have the departure and arrival times t_i^d and t_i^a , $1 \leq i \leq m$, respectively, and range R_i km. Let $t^{LU} > 0$ denote the amount of time needed to board/de-board the passengers of an e-AC. Let $t^{BS} > 0$ denote the period of time needed to swap a battery. Let q_i^S and q_i^E be the battery SOC at the start and end of mission i , respectively, with $q_i^S, q_i^E \leq Q$. We assume a battery safety margin $SF = 0.2Q$ such that it is always the case that $q_i^E \geq 0.2Q$ (20% safety margin). Let q_i^R be the minimum energy needed to perform mission i of range R_i (without a safety margin). Let P^C be the nominal power of charge at a charging station. Let q_{ij}^C be the battery capacity required to charge between two consecutive missions i and j , with q_{ij}^C a function of q_i^R and q_i^E , as we will show below. Finally, let t_{ij}^C denote the battery charging time needed to ensure sufficient energy for mission j , given that mission i is immediately succeeded by mission j . We define t_{ij}^C to be a function of q_i^S , q_i^E , q_i^R and P^C , as we will show below. Here, t_{ij}^C assumes a bi-linear profile: it increases linearly with a given slope when charging up to 90% of the battery capacity (fast charging), while for charging 90% or more of the battery capacity, the slope decreases significantly (slow charging), see Fig. 5.

Formally, we define the time to charge between missions i and j as follows:

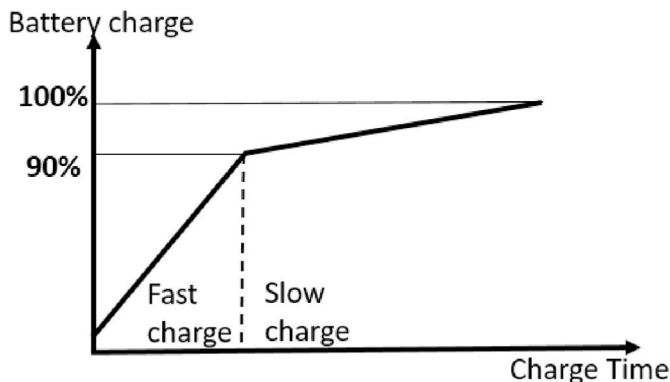


Fig. 5. Bi-linear charging profile.

$$t_{ij}^C = \begin{cases} \frac{q_{ij}^C}{P^C}, & \text{if } q_i^E < 0.9Q, q_j^S < 0.9Q \\ \frac{q_{ij}^C}{P^C/10}, & \text{if } q_i^E > 0.9Q, q_j^S > 0.9Q, \forall i, j \in M; i < j. \\ \frac{0.9Q - q_i^E}{P^C} + \frac{q_j^R + SF - 0.9Q}{P^C/10}, & \text{if } q_i^E < 0.9Q, q_j^S > 0.9Q \end{cases} \quad (1)$$

4.1.1. Decision variables

We considered the following decision variables:

$$\begin{aligned} x_{ik} &= \begin{cases} 1, & \text{if e-AC } k \text{ is assigned to mission } i \\ 0, & \text{otherwise} \end{cases} \\ y_k &= \begin{cases} 1, & \text{if e-AC } k \text{ is used at least once during the planning horizon} \\ 0, & \text{otherwise} \end{cases} \\ z_{ijk} &= \begin{cases} 1, & \text{if e-AC } k \text{ executes mission } j \text{ immediately after mission } i \\ 0, & \text{otherwise} \end{cases} \\ w_{ij}^{BS} &= \begin{cases} 1, & \text{if e-AC swaps batteries between consecutive missions } i \text{ and } j \\ 0, & \text{otherwise} \end{cases} \\ w_{ij}^{BC} &= \begin{cases} 1, & \text{if e-AC charges batteries between consecutive missions } i \text{ and } j \\ 0, & \text{otherwise.} \end{cases} \end{aligned}$$

we note that all missions considered are ordered by their t_i^d , $i \in M$, such that every two missions i and j where $i > j$, leads to $z_{ijk} = 0$. We also construct the following auxiliary variables:

$$\begin{aligned} a_{ij} &= \begin{cases} 1, & \text{if } w_{ij}^{BC} = 1 \text{ and } q_j^R + SF \geq 0.9Q \\ 0, & \text{otherwise} \end{cases} \\ b_{ij} &= \begin{cases} 1, & \text{if } a_{ij} = 1 \text{ and } q_i^E \geq 0.9Q \\ 0, & \text{otherwise} \end{cases} \\ c_{ij} &= \begin{cases} 1, & \text{if } a_{ij} = 1 \text{ and } b_{ij} = 0 \\ 0, & \text{otherwise,} \end{cases} \end{aligned}$$

with variable a_{ij} showing the case when only slow charge is needed, variable b_{ij} showing the case when only fast charging is needed and, variable c_{ij} showing the case when both fast and possibly slow charging is needed.

4.1.2. Objective function

We consider the cost c^{AC} of acquiring an e-AC, the cost c^{BS} of acquiring a battery, and the cost c^{BC} of charging a battery, where $c^{AC} \gg$

$c^{BS} \gg c^{BC}$. In this phase, the objective of the problem is to create a cost-efficient schedule for all e-AC, i.e., we minimize the acquisition cost of e-AC and spare batteries costs, as well as the operating cost associated with the electricity cost of charging a battery. Moreover, we also incur a large penalty, $H \gg c^{AC}$, for every unfulfilled mission. Thus, we consider the following objective function:

$$\min \sum_{k \in V} c^{AC} \cdot y_k + \sum_{i \in M} \left[\left(1 - \sum_{k \in V} x_{ik} \right) \cdot H + \sum_{j \in M} (\omega_{ij}^{BC} \cdot c^{BC} + \omega_{ij}^{BS} \cdot c^{BS}) \right], \quad (2)$$

where the first term corresponds to the minimization of e-AC acquisition costs by minimizing the number of e-AC used to carry out the missions, the second term attributes a large penalty H to each unassigned mission and, lastly, the third term minimizes the cost of battery charging and swapping.

4.1.3. Constraints

We consider the following constraints.

$$\sum_{k \in V} x_{ik} \leq 1, \forall i \in M \quad (3)$$

$$x_{jk} \geq \sum_{i \in M, i < j} z_{ijk}, \forall j \in M; k \in V \quad (4)$$

$$x_{ik} \geq \sum_{j \in M, i < j} z_{ijk}, \forall i \in M; k \in V \quad (5)$$

$$z_{ijk} \geq x_{ik} + x_{jk} - 1 - \sum_{l \in M, i < l < j} z_{ilk}, \forall i, j \in M; k \in V; i < j \quad (6)$$

$$\sum_{k \in V} y_k \leq \nu \quad (7)$$

$$\sum_{i \in M} x_{ik} \leq m \cdot y_k, \forall k \in V \quad (8)$$

$$\left(1 - \sum_{k \in V} z_{ijk} \right) \cdot H \geq t_i^d + t^{LU} + \omega_{ij}^{BS} \cdot t^{BS} + \omega_{ij}^{BC} \cdot t_{ij}^C - t_j^d, \forall i, j \in M; i < j \quad (9)$$

$$\omega_{ij}^{BS} + \omega_{ij}^{BC} \leq \sum_{k \in V} z_{ijk}, \forall i, j \in M; i < j \quad (10)$$

$$q_j^S = \left(1 - \sum_{k \in V} \sum_{i \in M, i < j} z_{ijk} \right) \cdot Q + \sum_{i \in M, i < j} \left[\omega_{ij}^{BS} \cdot Q + \omega_{ij}^{BC} \cdot (q_j^R + SF) + \left(\sum_{k \in V} z_{ijk} - \omega_{ij}^{BS} - \omega_{ij}^{BC} \right) \cdot q_i^E \right], \forall j \in M \quad (11)$$

$$q_i^E = q_i^S - q_i^R, \forall i \in M \quad (12)$$

$$q_{ij}^C = \begin{cases} q_j^R + SF - q_i^E, & \text{if } \omega_{ij}^{BC} = 1, \\ 0, & \text{otherwise} \end{cases}, \forall i, j \in M; i < j \quad (13)$$

$$a_{ij} \geq \frac{q_j^R + SF - 0.9 \cdot Q}{Q} - H \cdot (1 - \omega_{ij}^{BC}), i, j \in M; i < j \quad (14)$$

$$a_{ij} \leq \frac{q_j^R + SF}{0.9 \cdot Q} + H \cdot (1 - \omega_{ij}^{BC}), i, j \in M; i < j \quad (15)$$

$$a_{ij} \leq \omega_{ij}^{BC}, i, j \in M; i < j \quad (16)$$

$$b_{ij} \geq \frac{q_i^E - 0.9 \cdot Q}{Q} - H \cdot (1 - a_{ij}), i, j \in M; i < j \quad (17)$$

$$b_{ij} \leq \frac{q_i^E}{0.9 \cdot Q} + H \cdot (1 - a_{ij}), i, j \in M; i < j \quad (18)$$

$$b_{ij} \leq a_{ij}, i, j \in M; i < j \quad (19)$$

$$c_{ij} = a_{ij} - b_{ij}, \forall i, j \in M; i < j \quad (20)$$

Lastly,

$$t_{ij}^C = \begin{cases} \frac{q_{ij}^C}{P^C}, & \text{if } a_{ij} = 0 \\ \frac{q_{ij}^C}{P^C / 10}, & \text{if } b_{ij} = 1, \forall i, j \in M; i < j \\ \frac{0.9Q - q_i^E}{P^C} + \frac{q_j^R + SF - 0.9Q}{P^C / 10}, & \text{if } c_{ij} = 1 \end{cases} \quad (21)$$

Constraint (3) ensures that each mission is executed by at most one aircraft. Constraints (4–5) ensure that each mission is immediately preceded and succeeded by at most one mission. Together with Constraint (6), this ensures that missions i and j are characterized as consecutive missions if, and only if, e-AC k is assigned to both missions and does not carry out any other mission in between. Constraints (7–8) determine the number of used aircraft does not exceed the number of available aircraft, and if an aircraft is used, respectively. Constraint (9) ensures that an aircraft can only execute mission j immediately after arriving from mission i not only if mission j starts after mission i is concluded, but also if the aircraft has sufficient time to carry out passenger loading and unloading and to fulfill its battery renewal needs. Constraint (10) ensures that battery renewal opportunities are only allowed between two consecutive missions. Constraint (11) defines that the battery capacity at the beginning of each mission j is Q if it is the e-AC's first mission of the day or if its battery has been swapped with a fully charged ones, $q_j^R + SF$ if the e-AC has been charged just enough to execute its next mission and, finally, q_i^E if the e-AC has enough battery capacity remaining from its previous mission to fulfill its next mission, thus not requiring any battery renewal process. Constraint (12) traces the remaining battery at the end of each mission. Constraint (13) determines the amount of battery capacity needed to be charged between missions i and j if battery renewal is needed and allowed. Constraints (14–16) check if the battery capacity after the charge is complete is higher than 90% of the total battery capacity Q . For charges that verify these conditions, constraints (17–19) determines if the battery capacity at the beginning of the charge process is higher than 90% of the total battery capacity Q . Constraint (20) assesses if the battery capacity at the beginning of the charge process is lower than 90% of Q but by the end of the process is higher than 90% of Q . Constraint (21) measures the charging time (in minutes) according to the type of charge conditions defined in Constraints (14–20).

We make the following remarks regarding the constraints above.

Remark 1: Let us assume that an e-AC is assigned to some missions 1, 2 and 4, in this order. Then missions 1 and 4 are not considered to be consecutive, since mission 2 is executed in-between. Constraint (6) for missions 2 and 4 determines that $z_{241} \geq x_{21} + x_{41} - 1 - z_{231} = 1 \Rightarrow z_{241} = 1$ since constraint (5) ensures that $z_{231} = 0$ because $x_{31} = 0$. Similarly, for missions 1 and 2, $z_{121} \geq x_{11} + x_{21} - 1 = 1 \Rightarrow z_{121} = 1$. On the other hand, for missions 1 and 4, $z_{141} \geq x_{11} + x_{41} - 1 - z_{121} - z_{131} = 0$ since mission 3 is not executed by the e-AC and missions 1 and 2 are consecutive missions. However, given that constraint (5) ensures that mission 1 only has one succeeding mission, $1 \geq z_{121} + z_{131} + z_{141} + \dots + z_{1m1}$, and that $z_{121} = 1$, then $z_{131} = z_{141} = \dots = z_{1m1} = 0$. Thus, even though e-AC executes both missions 1 and 4, these are not consecutive.

Remark 2: Let us consider that mission 5 has the arrival time at the airport at 10:00, and mission 6 has the departure time at 11:00 from the airport. According to constraint (9), $(1 - \sum_{k \in V} z_{56k}) \cdot H \geq 15 + 20 \cdot \omega_{56}^{BS} + 60 \cdot \omega_{56}^{BC} \cdot t^{BC} - 60$. Here, t^{BC} is expressed in hours, and the time to board/

un-board is $t^{LU} = 15\text{min}$. If, in order to perform mission 6 after executing mission 5, this e-AC has to charge for 50 min ($t^{BC} = 0.83$), then $(1 - \sum_{k \in \mathcal{V}_{56k}} \cdot H) \geq 5$. Hence, to comply with constraint (9), $\sum_{k \in \mathcal{V}_{56k}} = 0$ so that $H \geq 5$. Therefore, missions 5 and 6 cannot be a consecutive pair of missions. However, if the time to charge is only 20 min, then $(1 - \sum_{k \in \mathcal{V}_{56k}} \cdot H) \geq -25 \Rightarrow \sum_{k \in \mathcal{V}_{56k}} \in \{0, 1\}$. Thus, in this case, even though the departure time of mission 6 is after the arrival time of missions 5, the two mission are not executed one immediately after the other.

Remark 3: We do not consider opportunistic charging, i.e., extra charging in-between flights. The main reason is that charging electrical batteries is expected to require a much larger period of time than fueling conventional aircraft, especially when charging extra the battery to a high SOC. Instead of opportunistic charging during the day, we ensure that all batteries (inside the aircraft and spares) are fully charged before the beginning of a day of operations (before first mission in the morning). In other words, we aim to charge fully during the night, rather than having time-consuming, extra charging in between flights.

4.1.4. Determining the size v of the e-AC fleet

The size v of the e-AC fleet is not known prior to optimization, so we determine v in an iterative manner as follows. We initialize $0 < v \ll m$ and check the value of the objective function in eq. (1) relative to H (see 4.1). If the objective function has the same order of magnitude as H , then it means that v is too small and there is an insufficient number of e-AC to carry out all m missions. In this case, we increment v and evaluate again the objective function. Otherwise, v is sufficiently large and we stop the iterative process.

4.1.5. Constraint linearization

In Section 4.1, constraints (9) and (11) are quadratic.

We linearize these constraints as follows. Consider a generic constraint $d = f \cdot E$, where f is a binary variable and E , $0 < E < \bar{E}$, is a continuous variable bounded below by \bar{E} . We linearize this constraint as follows (Torres, 1990):

$$d \leq \bar{E} \cdot f \quad (22)$$

$$d \leq E \quad (23)$$

$$d \geq E - (1 - f) \cdot \bar{E} \quad (24)$$

$$d \geq 0 \quad (25)$$

We note that if $f = 0$ in eq. (22), then $d = 0$. Also, eq. (24) states that d must be greater than a negative number. However, if $f = 1$, then eq. (22) ensures that $d < \bar{E}$, which is further tightened by eq. (23). Equation (25) ensures that $d \geq 0$ in all cases.

Following the example above, constraint (9) is linearized, using $d = \delta_{ij} = \omega_{ij}^{BC} \cdot t_{ij}^C$, as follows:

$$\left(1 - \sum_{k \in \mathcal{V}} z_{ijk}\right) \cdot H \geq t_i^a + t^{LU} + \omega_{ij}^{BS} \cdot t_i^{BS} + 60 \cdot \delta_{ij} - t_j^d \quad (26)$$

$$\delta_{ij} \leq t^{MAX} \cdot \omega_{ij}^{BC} \quad (27)$$

$$\delta_{ij} \leq t_{ij}^C \quad (28)$$

$$\delta_{ij} \geq t_{ij}^C - (1 - \omega_{ij}^{BC}) \cdot t^{MAX} \quad (29)$$

$$\delta_{ij} \geq 0 \quad (30)$$

Similarly, constraint (11) is linearized, using $d = \mu_{ij} = (\sum_{k \in \mathcal{V}} z_{ijk} - \omega_{ij}^{BS} - \omega_{ij}^{BC}) \cdot q_{ij}^E = \gamma_{ij} \cdot q_{ij}^E$, as follows:

$$q_{ij}^S = \left(1 - \sum_{k \in \mathcal{V}} \sum_{i \in \mathcal{M}} \sum_{i < j} z_{ijk}\right) \cdot Q + \sum_{i \in \mathcal{M}} \sum_{i < j} [\omega_{ij}^{BS} \cdot Q + \omega_{ij}^{BC} \cdot (q_j^R + SF) + \mu_{ij}] \quad (31)$$

$$\gamma_{ij} = \sum_{k \in \mathcal{V}} z_{ijk} - \omega_{ij}^{BS} - \omega_{ij}^{BC} \quad (32)$$

$$\mu_{ij} \leq \gamma_{ij} \cdot H \quad (33)$$

$$\mu_{ij} \leq q_i^E \quad (34)$$

$$\mu_{ij} \geq q_i^E - (1 - \gamma_{ij}) \cdot H \quad (35)$$

$$\mu_{ij} \geq 0 \quad (36)$$

Also, in Section 4.1, constraints (13) and (21) are indicator functions. We also linearize constraints (13) as follows:

$$q_{ij}^C \geq q_j^R + SF - q_i^E - (1 - \omega_{ij}^{BC}) \cdot H \quad (37)$$

$$q_{ij}^C \leq q_j^R + SF - q_i^E + (1 - \omega_{ij}^{BC}) \cdot H \quad (38)$$

Constraint (37) and (38) ensure that when ω_{ij}^{BC} is 1, $q_{ij}^C \geq q_j^R + SF - q_i^E$. Contrarily, when $\omega_{ij}^{BC} = 0$, then $-H \leq q_{ij}^C \leq H$, indicating that q_{ij}^C can assume any value as long as its absolute value is bounded by H . However, constraint (13) also establishes that if $\omega_{ij}^{BC} = 0$, then q_{ij}^C is necessarily 0 as well, therefore the linearized set of constraints also include the following inequality:

$$q_{ij}^C \leq \omega_{ij}^{BC} \cdot H \quad (39)$$

Similarly, constraint (21) is linearized as follows:

$$t_{ij}^C \geq \frac{q_{ij}^C}{PC} - H \cdot a_{ij} \quad (40)$$

$$t_{ij}^C \leq \frac{q_{ij}^C}{PC} + H \cdot a_{ij} \quad (41)$$

$$t_{ij}^C \geq \frac{q_{ij}^C}{PC/10} - (1 - b_{ij}) \cdot H \quad (42)$$

$$t_{ij}^C \leq \frac{q_{ij}^C}{PC/10} + (1 - b_{ij}) \cdot H \quad (43)$$

$$t_{ij}^C \geq \frac{0.9Q - q_i^E}{PC} + \frac{q_j^R + SF - 0.9Q}{PC/10} - (1 - c_{ij}) \cdot H \quad (44)$$

$$t_{ij}^C \leq \frac{0.9Q - q_i^E}{PC} + \frac{q_j^R + SF - 0.9Q}{PC/10} + (1 - c_{ij}) \cdot H \quad (45)$$

As an example, when $a_{ij} = 0$, constraints (17–20) establishes that both $b_{ij} = 0$ and $c_{ij} = 0$. Consequently, constraints (42–45) ensure that $-H \leq t_{ij}^C \leq H$, while constraints (40) and (41) ensure that $t_{ij}^C = \frac{q_{ij}^C}{PC}$, which is in line with constraint (21).

4.2. Second phase: optimal time for battery charge and minimizing the number of charging stations and batteries

In this second phase, we consider as input the battery-charging and swapping events planned in the first phase. Also, in contrast with the first phase model, we now consider a discrete-time optimization model. Our aim is to determine the optimum moment when a battery charge starts such that the total number of charging stations and spare batteries is minimized.

We consider a discrete time horizon of T time units. Let C_S denote the set of identical charging stations, $|C_S| = c_s$, that have to fulfill all charging events C_E , $|C_E| = c_e$. Let C_{ES} denote the set of swapping battery events, $|C_{ES}| = c_{es}$ and $C_{ES} \subset C_E$. Let T_S denote the set of time units when battery swaps are carried out. We define

$$s^t = \begin{cases} 1, & \text{if } t \in T_S \\ 0, & \text{if } t \in T \setminus T_S. \end{cases}$$

Let an event $n \in C_E$ have a duration $d_n = t_{ij}^c$ (determined in phase 1). Let $[e_n, l_n]$ define a time window within which event n needs to start. If $w_{ij}^{BC} = 1$ (battery charging at a charging station), then $e_n = t_i^a$ and $l_n = t_j^d - d_n$. If $w_{ij}^{BS} = 1$ (battery swap), then $e_n = t_i^a$ and $l_n = T$.

4.2.1. Decision variables

We considered the following decision variables:

$$o_k^t = \begin{cases} 1, & \text{if charging station } k \text{ is in service at time } t \\ 0, & \text{otherwise} \end{cases} \quad (46)$$

$$u_{ik}^t = \begin{cases} 1, & \text{if charging station } k \text{ starts servicing event } i \text{ at time } t \\ 0, & \text{otherwise} \end{cases} \quad (47)$$

$$r_k = \begin{cases} 1, & \text{if charging station } k \text{ is used at least once during planning horizon } T \\ 0, & \text{otherwise} \end{cases} \quad (48)$$

we also define the following auxiliary variables:

$b \in \mathbb{N}^+$: Number of batteries needed in stock to fulfill every swap requirement.

$p^t \in \mathbb{N}^+$: Number of swapped batteries that at time t are waiting to be charged.

4.2.2. Objective function

The goal of the second phase of the problem consists in minimizing the number of spare batteries, b , and the number of charging stations, r_k , $k \in C_S$, as follows:

$$\min \left(b + \sum_{k \in C_S} r_k \right) \quad (49)$$

4.2.3. Constraints

We considered the following constraints:

$$\sum_{k \in C_S} \sum_{t=e_i}^{l_i} u_{ik}^t = 1, \quad \forall i \in C_E \quad (50)$$

$$o_k^t = \sum_{i \in C_E} \sum_{\substack{h=t-d_i \\ h \geq e_i}}^t u_{ik}^h, \quad \forall t \in T; k \in C_S \quad (51)$$

$$p^t = \sum_{\substack{t' \in T_S \\ t' \leq t}} s^{t'} - \sum_{i \in C_{ES}} \sum_{k \in C_S} \sum_{\substack{t'' \in T \\ e_i \leq t'' \leq t-d_i}} u_{ik}^{t''}, \quad \forall t \in T_S \quad (52)$$

$$b = \max(\{p^t, p^t, \dots, p^t\}), \quad \forall t, t', \dots, t'' \in T_S \quad (53)$$

$$\sum_{i \in C_E} \sum_{t \in T} u_{ik}^t \leq c_e \cdot r_k \quad (54)$$

$$\sum_{k \in C_S} r_k \leq c_s \quad (55)$$

Constraint (50) guarantees that every charging event must be satisfied by exactly one charging station within its window $[e_i, l_i]$. Constraint

(51) ensures that each battery recharge is carried out continuously by the same charging station. Constraint (52) determines the number of swapped batteries awaiting to be charged whenever a new swap occurs. Constraint (53) determines the number of batteries required in stock to comply with the swaps conducted throughout the planning horizon T . Constraints (54–55) assess if a charging station is used and ensure that the number of used charging stations cannot exceed the number of available charging stations, respectively. Constraint (53) can be linearized by, for instance, introducing additional indicator variables $\delta_{ij} = 1$ if $p_{ij} > b, t_i \in T_S$, see [MirHassani and Hooshmand \(2019\)](#), Chapters 4.5 and 4.6. Specifically, our initial constraint can be formulated as: $b > = p_{ij}, j \in \{1, \dots, n\}, b < = p_{ij} + M \cdot (1 - \delta_{ij}), j \in \{1, \dots, n\}, \sum_{j=1}^n \delta_{ij} = 1$.

We make the following remarks regarding the constraints above.

Remark 4: Let us consider the case when an e-AC arrives at $t^a = 100$ and departs at $t^d = 200$ from two consecutive missions. During the turnaround time, this e-AC is required to charge for 30min to renew its battery before departing again. Thus, for this charging event i , $e_i = 100$ and $l_i = 170$. Constraint (50) ensures that charging event i occurs within $t = 100$ and $t = 170$. Assuming that this charging event is done at charging station k at $t = 150$, $u_{ik}^{150} = 1$, then constraint (51) guarantees that the charging is performed without interruptions.

Remark 5: We consider that a depleted battery is swapped with a fully charged one. The swapped depleted battery can be charged and reused again. Thus, the number of swapped batteries waiting to be charged, p^t , can increase or decrease with t . Constraint (52) determines the number of swapped batteries that are waiting to be charged by subtracting the number of swaps until time t (inclusive) with the number of swapped batteries that have already been charged and are apt to replace depleted ones.

4.2.4. Initializing the number of charging stations

The number of charging stations c_s available is not known prior to the optimization, and it is determined in an iterative manner as follows. The solution obtained in phase 1 assumes that all charging and swapping events are fulfilled. Thus, the solution of the model in phase 2 must cover all charging events obtained by the phase 1 model. Thus, we initialize $0 < c_s \ll v$ and increment c_s until we obtain a feasible solution for the phase 2 model.

5. e-Aircraft and battery models

In this section, we discuss the models used to estimate i) the battery SOC decrease due to the completion of a mission i of range R_i , and ii) the charging time t_{ij}^c needed for the battery to be able to carry out mission j of range R_j immediately after mission i . Lastly, since there are not yet available charging specifications for electric or hybrid-electric short-range flights, we introduce an electrified version of a conventional narrow-body aircraft, Embraer 175, who is usually used for short-range flights and whose characteristics are recalculated to account for possible weight penalties given by the installation of batteries instead of fuel.

5.1. Aircraft model

The energy required to execute a mission of range R is calculated by means of the Mission Analysis methods, widely used during conceptual and preliminary aircraft design to estimate the fuel needed to carry out a nominal mission. This method uses a weight fraction method ([Raymer, 1992](#)) together with a Breguet formula ([Hepperle, 2012](#)) that have been properly adapted to take into account the differences between electric and conventional propulsion configurations. The rationale behind the aforementioned approach consists into determining the amount of fuel for a conventional aircraft and then calculating the correspondent amount of electrical energy needed in case of an e-AC.

Specifically, we take the following steps. First, the mission is considered to be composed of the following phases: takeoff, climb,

cruise, descent and landing. During descent and landing, we assume that the requested energy is negligible.

Second, in line with the weight fraction method (Raymer, 1992), it is assumed that a conventional aircraft burns 7% of its Maximum Take Off Weight (MTOW) during Take-Off and Climb segments. Thus, the correspondent electrical energy is calculated as follows:

$$\xi_b^{TO,CL} = \frac{W_f \cdot E_f^* \cdot \eta_f}{\eta_b} = \frac{(1 - 0.93) \cdot MTOW \cdot E_f^* \cdot \eta_f}{\eta_b}, \quad (56)$$

where E_f^* denotes the specific energy density of the fuel, η_f and η_b the fuel and battery to propulsive power efficiency, respectively, and W_f the fuel mass.

Third, the total energy that needs to be provided by the batteries of the e-AC during cruises is estimated using the Breguet Formula adapted to an e-AC (Hepperle, 2012) as follows:

$$\xi_b^{CR} = E_b^* \cdot W_b = \frac{R \cdot g}{\eta_b \cdot L/D} \cdot MTOW, \quad (57)$$

where E_b^* denotes the specific energy density of the battery, W_b is the battery mass, R is the flight range, g is the gravity acceleration, and L/D is the lift to drag ratio.

Combining eq. (56) and eq. (57) it follows that the battery energy needed to perform a mission of range R , is:

$$\xi_b = \xi_b^{TO,CL} + \xi_b^{CR} = \left((1 - 0.93) \cdot E_f^* \cdot \eta_f + \frac{R \cdot g}{L/D} \right) \cdot \frac{MTOW}{\eta_b}. \quad (58)$$

We note that, for a given electrical technology (for which correspondent values of battery specific energy E_b^* and electrical efficiency η_b are determined) and for a given aircraft (assuming a value for the aerodynamic characteristics expressed by L/D) the requested energy, is linearly depending on the mission range (see also the right graph in Fig. 6 where $E_f^* = 11,000 \text{ Wh/kg}$, $\eta_b = 73\%$ and $\eta_f = 33\%$ and $L/D = 16.5$). We also note that for short ranges the required energy is still relatively high because of the energy needed to perform take-off and climb. Lastly, the MTOW has been calculated using an iterative class I estimation method (Raymer, 1992) as explained in detail in Section 5.3.

5.2. Battery charge model

The charging model is used to calculate the charging time in such a

way that an aircraft that just completed mission i of range R_i can immediately perform mission j of range R_j . The charging time depends on the nominal power of charge P_C , which is defined as follows:

$$P^C = \frac{P_{MAX}^D}{C^{MAX}/C^{NOM}}, \quad (59)$$

where C^{MAX} and C^{NOM} are the C-rates at which the discharge and nominal charge occur, respectively. A C-rate is a measure of the rate at which a battery charges/discharges relative to its nominal capacity. In this paper, we assume that $C^{MAX} = 6$ and $C^{NOM} = 1$, where the chosen values reflect typical charging and discharging conditions for a Li-Ion battery.

We also assume that the maximum power required for takeoff is proportional to the MTOW of the aircraft considering the value extracted from the reference aircraft (see Table 1). In addition, the charging time follows a bi-linear dependence on the battery State of Charge (SOC), as expressed in eq. (21); this relation takes into account two different charging phases (constant current and constant voltage).

Fig. 6 shows how the energy consumption is determined based on the range to be flown for mission j of range R_j which immediately follows after mission i of range R_i . Next, this energy is used to determine the time to charge this energy.

Using the model in Section 5.1 the amount of energy (expressed in SOC) needed for missions i and j is determined. When the aircraft completes mission i , its final SOC is SOC_i . For the new range R_j , a new SOC is required, SOC_j . Then the energy to charge is given by $SOC_j - SOC_i$. The SOC is defined as the ratio of the energy level of the system (the aircraft) at a certain moment ξ , over the maximum energy that the system can store ξ_{max} , i.e.,

Table 1
Embraer E175 and e-AC weight parameters.

Parameter	Embraer E175	e-AC
W_{pay} (Kg)	10,094	10,094
$MTOW$ (Kg)	40,370	54,660
EOW (Kg)	21,886	28,558
W_{energy} (Kg)	9,355	16,008
Battery Capacity (KWh)	–	12,804
Take Off Power (MW)	14.5	22.65

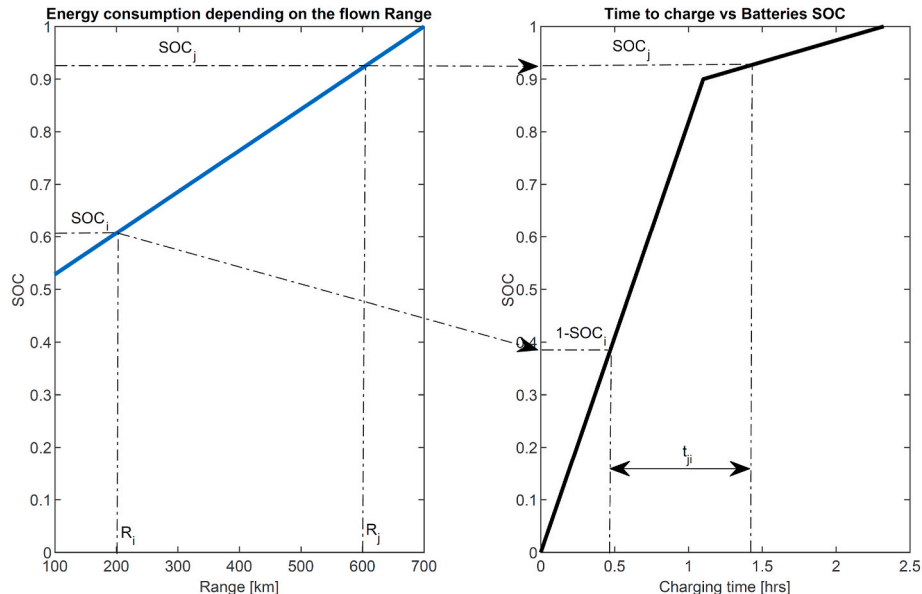


Fig. 6. Procedure to determine the time-to-charge t_{ij}^C .

$$SOC = \frac{\xi}{\xi_{\max}}$$

In other words, $SOC = 1$ when the aircraft start a mission with fully charged batteries, whereas $1 < SOC < 0$ when an aircraft lands after the completion of a certain mission. For the present study, it is thus necessary to adopt a model to correlate the SOC of a certain aircraft to the mission that the aircraft itself has flown. As such, eqs. (56)-(58) determine the relation between the SOC and the flown range R of the aircraft: for a full electric aircraft, this relation is linear and it is represented in the left graph of Fig. 6, i.e. $\xi = A + B \cdot R$, where A and B are two coefficients depending on the technical performance of the aircraft.

Lastly, the time needed to charge is determined using a bi-linear charging function (see the right graph of Fig. 6).

5.3. e-Aircraft class I estimation

An initial set of aircraft characteristics is needed to initialize the calculations introduced in Sections 5.1 and 5.2. Since currently there are no fully e-AC that can be taken as reference for regional transportation, a modified class I estimation method is applied to an existing aircraft to estimate the new $MTOW$, where the battery is the main propulsive energy source. The method consists in including eq. (58) as mission analysis to estimate the weight of the needed batteries, into an iteration loop (Raymer, 1992) to estimate a converged value of the $MTOW$.

Table 1 shows the results of the iterative class I estimation loop. The $MTOW$ of the electrified version increases of about 35% compared to the baseline aircraft, despite of a drastic reduction of the nominal range. In fact it is assumed that the e-AC can fly a nominal range of 700 Km whereas the reference E175 has a range of approximately 4000 km. This difference is mainly caused by the very low specific energy density of the batteries when compared to the fuel.

6. Numerical results

In this section we illustrate the performance of our two-phase optimization model for 49 short-range missions, i.e. 49 round-trip flights, that arrive at and depart from Amsterdam Airport Schiphol (AMS) during one day of operations and have a range of at most 350 km one way from AMS. Fig. 7 shows the number of missions occurring simultaneously during the day. The optimization model is solved with Gurobi 8.1.1 with standard settings, on an Intel Core i7-5500U, 2.50 GHz. The results are obtained in 42min. To linearize constraint (53), we consider the function $\text{Model.addGenConstrMax}()$, which introduces additional slack variable for linearization, see Gurobi (2021). The routine $\text{Model.addGenConstrMax}()$, introduces additional slack variable δ_j , $j \in \{1, \dots, n\}$ and slack variable z_j , $j \in \{1, \dots, n\}$ to linearize a constraint $w = \max(x_1, x_2, \dots, x_n)$ as follows: $w = x_j + \delta_j$, $j \in \{1, \dots, n\}$, $z_1 + \dots + z_j = 1$, $SOS1(s_j, z_j)$, $j \in \{1, \dots, n\}$, $s_j > 0$, $j \in \{1, \dots, n\}$, $z_j \in \{0, 1\}$, $j \in \{1, \dots, n\}$. The SOS1 constraints state that at most one of the two variables δ_j and z_j can be non-zero, which models the implication $z_j = 1 \rightarrow s_j = 0$.

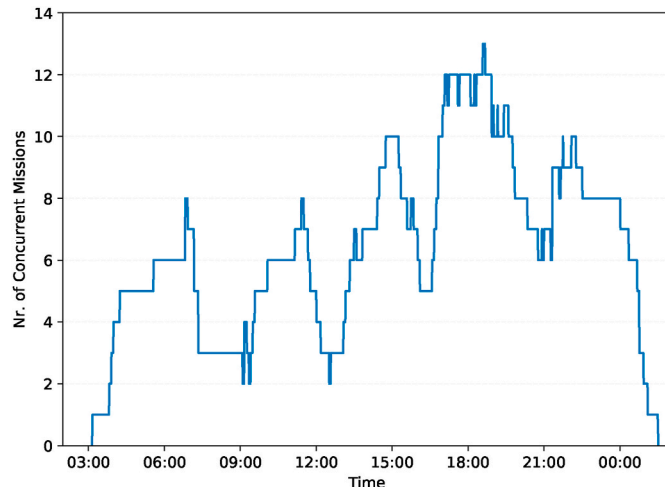


Fig. 7. Missions to and from AMS during one day of operations.

6.1. Estimation of model parameters

In estimating the model parameters for the e-AC, we consider as reference the electric aircraft Pipistrel Taurus Electro G2 (Pipistrel, 2018) and the conventional, regional aircraft Embraer E175.

The acquisition cost and the battery price of Pipistrel Taurus Electro G2 with a 9.7 KWh battery, was in 2018, 10,619€/KWh and 1,402€/KWh (Pipistrel, 2018), respectively. Furthermore, considering Netherlands' electricity price for transportation purposes in 2018, recharging a battery costs 0.083€/KWh. Thus, considering the 8,004 KWh battery capacity of the Embraer E175 electric version shown in Table 1, we assume that the cost of the aircraft acquisition, of the battery purchase and of the battery recharge (from depleted to fully charged) are 85×10^6 €, 11×10^6 € and 664 €, respectively. Given that cost for an Embraer E175 is approximately 42×10^6 € (FlightGlobal, 2017; Airways, 2018) and that electric propulsion is more expensive than conventional propulsion, we assume a cost of 85×10^6 € for an electrical aircraft. Without loss of generality, we scale all costs above by a factor 1/664.

For the model in Section 4.1 we assume a constant duration of 20min for battery swap, and a 15min duration for loading and unloading of passenger in the e-AC.

6.1.1. e-Ac fleet sizing, mission and battery renewal schedule

Fig. 8 shows an optimal e-AC-to-mission schedule where a fleet of 15 e-AC, 23 battery charges and 9 battery swaps are needed to fulfill all the 49 missions considered (see Fig. 7). These results are obtained with the optimization models in Section 4.1 and Section 4.2.

During the busiest time of the day, from 18:30–19:30, there are 13 missions being executed at the same time (see Fig. 7). However, the obtained schedule (see Fig. 8) shows that during this busy period, two additional e-AC are needed, having a total need of 15 electric aircraft. This is due to the fact that, during this period, two e-AC are undergoing battery renewal procedures, and, consequently, cannot be assigned to any mission. Furthermore, Fig. 8 shows that battery-swapping occurs only during the second half of the day (from 15:00 onwards), while battery-charging events occur evenly throughout the day. There are no battery charging or swapping early on since we assume that all batteries are fully charged at the beginning of the day.

6.1.2. Charging stations and swap battery infrastructure requirements for the e-AC

Fig. 8 shows that the e-AC schedule requires 24 battery charges (light blue lines) and 9 battery swaps (orange lines). Fig. 9a shows the time windows i.e., the time between two consecutive missions during which a battery charge/swap event is scheduled (the output of phase 1 Optimization) versus the actual period when these 24 + 9 charging events take place. Towards the end of the day, the swapped batteries become depleted. Our model ensures that all batteries are fully charged at the beginning of a new day of operations (before the first mission of the day). As a result, although there are no more missions in the last phase of the day to require battery charging, the depleted swap batteries are required to charge before the beginning of the day. During night, the time windows are larger since the turnaround time until next mission in the morning is larger. The charge of the swapped batteries is pushed towards the end of the day, where the time windows are larger. This shows that battery swapping is used in the last phase of the day, when the number of flights increases significantly and the number of charging stations is not large enough to support the simultaneous charging

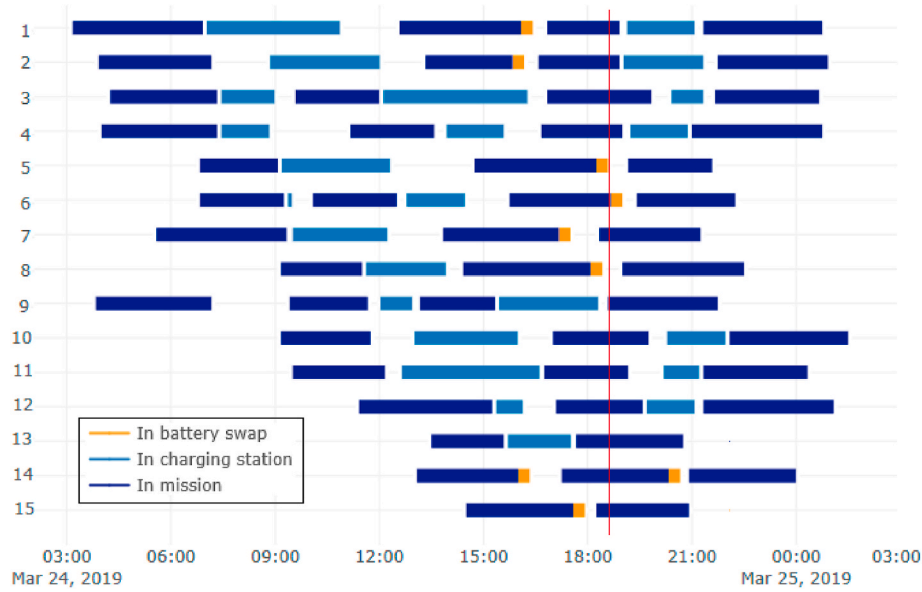


Fig. 8. Optimal fleet schedule when considering 49 missions. A total of 15 e-AC are needed to carry out all the 49 missions. A vertical red line indicates the peak time when 13 aircraft are executed at the same time. (For interpretation of the references to colour in this figure legend, the reader is referred to the Web version of this article.)

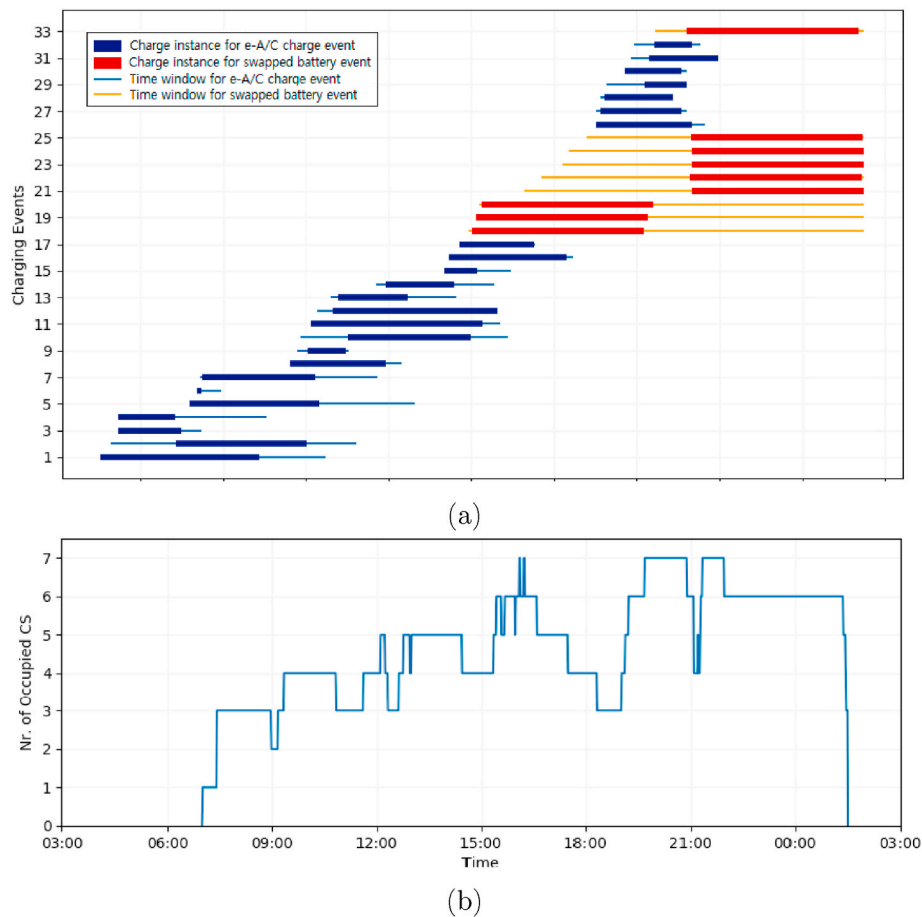


Fig. 9. (a) Time window and actual charging instances of charging events either originating in e-AC charges or swapped batteries charges. (b) Number of charging stations working simultaneously.

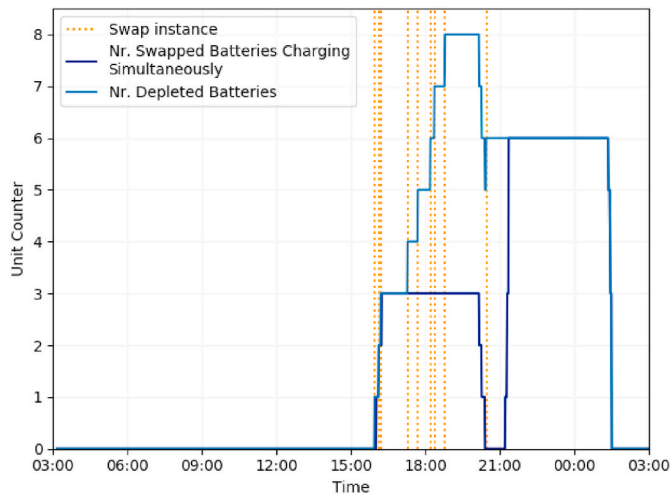


Fig. 10. Impact of battery swaps and its charging moments on the number of depleted batteries.

needed during this peak period.

Regarding the infrastructure needed to support these electric flights, Fig. 9a shows that a minimum of 7 charging stations need to be available at the airport. This is because, irrespective of the actual charging period, events 26 through 32 will always overlap, given their limited time window. Furthermore, at 20:45, a total of 16 events need to be simultaneously processed. However, only 7 are performed using a charging station. This illustrates that the charging events are arranged so that a minimal number of charging stations is used in the charging process. Fig. 9a also shows that a mix of charging the batteries at a station and battery swaps is preferred in the second part of the day, when the number of simultaneous missions increases.

Fig. 9b shows the number of charging stations (CS) that are in service at the same time. The charging stations are particularly busy at the end of the day since batteries that were previously used for swaps are now also re-charged at a charging station. These events have a wider time window than charging events originated from battery charges, therefore they offer a bigger schedule flexibility. Accordingly, in order to minimize the number of charging stations operating at the same time, charging events originating from battery swaps are postponed to less busy periods, i.e., periods of the day with less demand from events generated by battery charges. This situation is particularly evident in events 21 through 25, which are delayed until events 26 to 30 are completed.

Figs. 8 and 9a show that a stock of 8 spare batteries are required to fulfill every swap need during one day of operations, with a total of 9 swaps being performed. In particular, Fig. 10 shows how the number of depleted batteries is impacted by the moments at which a battery swap occurs (swap instances) as well as the charging events of these batteries. Here, the number of spare batteries is driven by two factors. To begin with, the first 8 swaps occur within a shorter time frame than the charging duration of these batteries. Thus, there is not sufficient time to fully charge the batteries so they can replace forthcoming swapped batteries. Second, the first 8 swaps occur during a period of high demand from events originated from battery charges. Hence, the charging of these swapped batteries is delayed so that the battery charges can be completed within their time window. As a result of this delay, the number of depleted batteries grows. These batteries become available later, so any swap that occurs in the meantime needs to be performed with a spare battery.

7. Conclusions

We have developed a two-phase optimization model that determines

the number of resources, i.e., number of electric aircraft, charging stations and spare batteries, required to fulfill a set of missions (round-trip flights). With this, we determined a schedule for electric aircraft to perform round-trip flights. Our approach considers as battery renewal options both swapping batteries with spare one, or charging batteries at a charging station. If the battery is charged at a charging station, then the charging duration is a function of the residual energy level of the battery and the range the aircraft is scheduled to fly next.

Our proposed model has been implemented for a set of short-range flights arriving and departing from a reference airport during a day of operations. The results show that a mix of using both charging stations and spare batteries can enable a fleet of electric aircraft to execute three times more round-trip flights than the size of this fleet. Moreover, the results show that charging the electric aircraft at a charging station is preferred in the first part of the day, while a mix of battery swapping and charging at a station is preferred in the second, more busy part of the day, where the number of missions performed at the same time increases. Nonetheless, although we consider the scheduling of electric aircraft as an application, our proposed model is generic and can be applied for hybrid-electric aircraft provided charging specifications are given, as well as for other electric means of transport, where the vehicle fleet sizing and logistics of vehicle charging are of interest.

As future work we plan to extend our analysis for a set of more complex types of missions that could involve several flight legs and detailed flight phases. Also, we plan to consider dedicated battery technologies to illustrate our models.

References

- Adler, J.D., Mirchandani, P.B., 2016. The vehicle scheduling problem for fleets with alternative-fuel vehicles. *Transport. Sci.* 51 (2), 441–456.
- Airways, 2018. American Airlines Purchases 15 Additional Embraer E175s.
- Chao, Z., Xiaohong, C., 2013. Optimizing battery electric bus transit vehicle scheduling with battery exchanging: model and case study. *Procedia-Social and Behavioral Sciences* 96, 2725–2736.
- Emde, S., Abedinnia, H., Glock, C.H., 2018. Scheduling electric vehicles making milk-runs for just-in-time delivery. *IIE Transactions* 50 (11), 1013–1025.
- FlightGlobal, 2017. American Airlines Has Placed a Firm Order for 10 Embraer E175 Jets.
- Gurobi, 2021. Gurobi.model.addgenconstrmax. https://www.gurobi.com/documentation/9.1/refman/py_model_agc_max.html. (Accessed 1 September 2021).
- Hepperle, M., 2012. Electric flight-potential and limitations. In: *Workshop on Energy Efficient Technologies and Concepts Operations*. STO-MP-AVT209.
- Justin, C.Y., Payan, A.P., Briceno, S.I., German, B.J., Mavris, D.N., 2020. Power optimized battery swap and recharge strategies for electric aircraft operations. *Transport. Res. C Emerg. Technol.* 115, 102605.
- Kleinbekman, I.C., Mitici, M., Wei, P., 2019. Rolling-horizon electric vertical takeoff and landing arrival scheduling for on-demand urban air mobility. *J. Aero. Inf. Syst.* 1–10.
- Lee, D.S., Fahey, D.W., Forster, P.M., Newton, P.J., Wit, R.C., Lim, L.L., Owen, B., Sausen, R., 2009. Aviation and global climate change in the 21st century. *Atmos. Environ.* 43 (22–23), 3520–3537.
- Li, J.-Q., 2013. Transit bus scheduling with limited energy. *Transport. Sci.* 48 (4), 521–539.
- MirHassani, S., Hooshmand, F., 2019. *Methods and Models in Mathematical Programming*. Springer.
- Pipistrel, 2018. Pipistrel Taurus Electro Price Lists.
- Raymer, D., 1992. *Aircraft Design: a Conceptual Approach*. American Institute of Aeronautics and Astronautics, Inc.
- Rinaldi, M., Parisi, F., Laskaris, G., D'Ariano, A., Viti, F., 2018. Optimal dispatching of electric and hybrid buses subject to scheduling and charging constraints. In: *Proceedings of the 21st International Conference on Intelligent Transportation Systems (ITSC)*. IEEE, pp. 41–46.
- Sun, B., Sun, X., Tsang, D.H., Whitt, W., 2019. Optimal battery purchasing and charging strategy at electric vehicle battery swap stations. *Eur. J. Oper. Res.* 279 (2), 524–539.
- Tamma, P., Schaart, E., Gurzu, A., 2020. Europe's Green Deal Plan Unveiled.
- Torres, F.E., 1990. Linearization of mixed-integer products. *Math. Program.* 49 (1), 427–428.
- Verma, A., 2018. Electric vehicle routing problem with time windows, recharging stations and battery swapping stations. *EURO Journal on Transportation and Logistics* 7 (4), 415–451.
- Wen, M., Linde, E., Ropke, S., Mirchandani, P., Larsen, A., 2016. An adaptive large neighborhood search heuristic for the electric vehicle scheduling problem. *Comput. Oper. Res.* 76, 73–83.